Filtered Multicarrier Transmission

Juha Yli-Kaakinen,[1] Markku Renfors,[1] and Eleftherios Kofidis[2,3]

[1]Tampere University, Department of Electrical Engineering, FI-33101, Tampere, P.O. Box 553, Finland
[2]University of Pireaus, Department of Statistics and Insurance Science, GR-18534, Pireaus, Greece
[3]Computer Technology Institute & Press "Diophantus" (CTI), GR-26504, Patras, Greece

Introduction

Multicarrier transmission technology is a cornerstone of the existing and emerging broadband wireless communication systems. While orthogonal frequency-division multiplexing (OFDM) is, by far, the most widely deployed multicarrier technology, a family of filtering-based multicarrier waveforms have also been widely investigated as candidates for future networks, targeting to relax certain critical limitations of it. Such a limitation, shared by all multicarrier schemes, is their high peak-to-average power ratio (PAPR) and its effect on the transmitter (TX) power amplifier efficiency. However, the main motivation for investigating *filtered* multicarrier schemes is the poor spectrum localization of OFDM signals. The resulting out-of-band (OOB) emissions introduce crosstalk between independently operated or differently parametrized OFDM multiplexes, unless relatively wide guard bands (GBs) are allocated between them. Fifth generation (5G) and beyond wireless networks are intended to support with high spectral efficiency various applications and services with quite different requirements for the physical layer. This demands high flexibility in the waveform parametrization and the high OOB emissions of OFDM become critical.

A wide variety of signal processing techniques have been proposed in the literature for suppressing the sidelobes of the OFDM spectrum. One obvious scheme among them is based on filtering the OFDM signal after generating it in the usual way. Traditionally, filtering is used in OFDM systems to reduce the needed GBs around frequency channels (or carriers) with fixed bandwidth. In more advanced scenarios, the filtering needs to be done dynamically for subbands with varying bandwidths and center frequencies, and this has not been considered realistic until recent times.

Another line of study is that of filter-bank multicarrier (FBMC) waveforms, which can reach excellent spectrum localization. However, when targeting to maximize the spectrum utilization with FBMC, it is necessary to use offset quadrature amplitude modulation (OQAM) for subcarriers to reach orthogonality. Due to the resulting inconveniences in the signal structure and the increase in computational complexity that FBMC entails, its practical use has so far been limited to certain specific applications only.

Wiley 5G Ref. Edited by Rahim Tafazolli, Chin-Liang Wang and Periklis Chatzimisios.
DOI: 10.1002/9781119471509.w5GRef002

Fundamentally, while FBMC applies filtering at the subcarrier level, filtered OFDM (F-OFDM) applies filtering for synchronously operated groups of subcarriers to avoid interference leakage between adjacent subbands. These subbands can then be allowed to operate asynchronously or each subband can use its own set of OFDM parameters. This is referred to as mixed-numerology operation. Basically, subband-level filtering is enough and may lead to lower computational complexity and power consumption than subcarrier-wise filtering. One important issue in this context is that sharp filtering of an OFDM signal harms the orthogonality of subcarriers, introducing in-band interference which may degrade the link performance unless the filtering scheme is carefully optimized.

In the following sections, the section titled "Multicarrier Waveforms with Well-Contained Spectrum" starts with a review of alternative techniques for enhancing OFDM spectrum, followed by a review of FBMC waveform basics. The section titled "Fast-Convolution Filter Bank" focuses on implementing filtering and filter banks (FBs) through fast Fourier transform (FFT)-domain processing, referred to as fast-convolution filter bank (FC-FB). This is found to be a flexible and efficient way for both FBMC and subband filtered cyclic prefix orthogonal frequency-division multiplexing (CP-OFDM) waveform processing. The main OFDM spectrum enhancement schemes considered in the fifth-generation new radio (5G NR) context are F-OFDM and windowed overlap-and-add (WOLA), which is based on time-domain windowing. These are discussed in the section titled "Enhanced OFDM for 5G New Radio" in more detail, including FC-based F-OFDM (FC-F-OFDM), as well as performance and complexity evaluations using the mixed-numerology OFDM parameters adopted for 5G NR.

Multicarrier Waveforms with Well-Contained Spectrum

Enhanced OFDM

The main drawback of the cyclic prefix (CP)-OFDM is the high OOB leakage stemming from the rectangular pulse shape of the time-domain waveform (Banelli et al., 2014). High spectral leakage induces interference between adjacent subbands in asynchronous transmission scenarios, which are widely considered for uplink (UL) communications, like massive machine-type communications (mMTC), and for dynamic opportunistic spectrum use scenarios of cognitive radio. The OOB leakage is also critical in mixed-numerology scenarios of 5G NR discussed in Section 3 below. This interference can be reduced by using sufficient GBs between subbands, but this would result in reduced spectral efficiency. Furthermore, there is a target to reduce the carrier-level GB overhead from 10 % in long-term evolution (LTE) closer to 1 % in 5G NR (3GPP, 2019b), which becomes complicated to achieve with traditional time-domain filtering techniques.

Various enhanced OFDM schemes have been proposed in the literature for solving the high OOB emission problem. These include adaptive symbol transition (Mahmoud and Arslan, 2008), cancellation carriers (Brandes et al., 2006), constellation

expansion (Pagadarai et al., 2008), polynomial cancellation coding (Panta and Armstrong, 2003; Kongara et al., 2019), subcarrier weighting (Cosovic et al., 2006), and precoding-based schemes (Chen et al., 2011; Dai et al., 2019). Two additional techniques, time-domain windowing and subband- or carrier-level filtering (Faulkner, 2000; Leyonhjelm and Faulkner, 2005) are mainly considered in the 5G NR context and they will get the main focus below.

Time-domain windowing, commonly referred to as WOLA in the 5G NR context, is a straightforward approach to the sidelobe suppression by smoothing the discontinuities at the OFDM symbol boundaries (Muschallik, 1996; Weiss et al., 2004; Beaulieu and Tan, 2007; Bala et al., 2013; Zayani et al., 2018; Qualcomm, 2015). This approach has a very low complexity and it can be applied also on the receiver (RX) side for suppressing interference leakage from adjacent channels. However, its effectiveness depends on the length of cyclic extensions of OFDM symbols, and there is an inevitable tradeoff between sidelobe suppression performance and overhead in the throughput. This tradeoff can be relaxed if longer window transitions are used close to the subband edges, while the center subcarriers have shorter window transition (Sahin and Arslan, 2011). As the overall cyclic extension length needs to be the same for all subcarriers, the effective CP length becomes shorter at the edge subcarriers. The center subcarriers have longer effective CP, and they can support users with longer channel delay spread. The drawbacks of such edge windowing include higher computational cost (two inverse fast Fourier transforms (IFFTs) are needed instead of a single one) and increased complexity in user scheduling to subcarriers. The application of WOLA in the 5G NR context will be discussed in more detail in Section 3.

F-OFDM, in general, is a collection of techniques used for improving the spectral localization of OFDM waveforms. These techniques include, among others, conventional time-domain filters (Vakilian et al., 2013; Zhang et al., 2015; Wang et al., 2017; Zhang et al., 2018; Chen et al., 2019), polyphase-discrete Fourier transform (DFT) FBs (Tonello, 2006; Zakaria and Le Ruyet, 2012; Li et al., 2014; Zayani et al., 2018), as well as fast-convolution (FC)-based approaches (Renfors et al., 2015). In F-OFDM, filtering is applied at the subband level, corresponding to one or multiple contiguous physical resource blocks (PRBs) with the same subcarrier spacing (SCS), while utilizing CP-OFDM waveform for the synchronous PRB groups. With spectrally well-localized subbands, the numerology on each subband can be adapted to suit the service requirements and also asynchronous transmissions within the same carrier can be supported in different subbands.

The drawback of all F-OFDM techniques, in general, is that aperiodic (linear) convolution compromises the CP budget by increasing the time dispersion of the transmitted waveform and, therefore, reduces the tolerance to the delay spread of the channel. Long processing delays, on the other hand, increase the overhead in link-direction switching in case of time-division duplex (TDD) operation. Furthermore, sharp filtering of the OFDM sidelobes harms the orthogonality of subcarriers, especially at the edges of the filtered subband, introducing in-band interference, and hence increasing the error vector magnitude (EVM).

The filter design for F-OFDM is a compromise between the time and frequency localization of the waveform, the orthogonality of the subcarriers, implementation complexity, as well as the latency of the processing. The application of F-OFDM in the 5G NR context will be discussed in more detail in Section 3.

Regarding the high-PAPR issue of multicarrier waveforms, DFT-precoded OFDM (also known as DFT-spread-OFDM (DFT-s-OFDM)) is available and widely used for reducing the PAPR in OFDM-based systems, especially for uplink transmission. The WOLA and F-OFDM schemes are directly applicable also for spectrum enhancement of these low-PAPR waveforms (Loulou et al., 2020).

Universally Filtered Multicarrier

Universally filtered multicarrier (UFMC) (also called universal filtered OFDM (UF-OFDM)) is basically also a F-OFDM scheme, but it makes use of the zero prefix (ZP)-OFDM signal structure, instead of CP (Vakilian et al., 2013). Like filtered CP-OFDM, it can be seen as a compromise between FBMC and OFDM in the sense that, applying the filtering over a group of subcarriers, the filter length (with respect to FBMC) and spectral leakage (with respect to OFDM) can be considerably reduced. In UFMC, N_{ACT} active subcarriers are divided into M subbands of $N_{\text{ACT},m} = N_{\text{ACT}}/M$ subcarriers each and these subbands are then filtered by a low-order finite impulse response (FIR) filter. The prototype filter design initially proposed for UFMC is based on the Dolph-Chebyshev window (Vakilian et al., 2013), however, the design is not restricted to this selection.

In UFMC TX processing, each subband is first converted to the time domain using the IFFT of size N_{OFDM}. The filter center frequency is adjusted based on the center frequency of each subband and each time-domain sequence is then filtered with a filter of length $N_{\text{FILT}} - 1$. These M filtered sequences are combined (summed) to form a UFMC symbol of length $N_{\text{OFDM}} + N_{\text{FILT}} - 1$. A ZP of length N_{FILT} is added to each symbol in order to prevent the inter-symbol interference (ISI) due to the filter transients.

The complexity of UFMC TX processing, in terms of real multiplications, when realized using time-domain (TD) convolution, is $C_{\text{TD-UFMC}} = M[4N_{\text{OFDM}}N_{\text{FILT}} + C_{\text{IFFT}}(N_{\text{OFDM}})]$ where $C_{\text{IFFT}}(N_{\text{OFDM}})$ is the number of real multiplications required by IFFT of length N_{OFDM}. When using the frequency-domain (FD) realization of the UFMC TX as proposed in (Wild and Schaich, 2015), the complexity reduces to $C_{\text{FD-UFMC}} = C_{\text{IFFT}}(2N_{\text{OFDM}}) + M[C_{\text{IFFT}}(L) + C_{\text{FFT}}(2L) + 12L] + 4(M-1)L$ real multiplications. Here $L > N_{\text{ACT},m}$ is the length of the short transform used for converting the $N_{\text{ACT},m}$ active subcarriers of each of the M subbands to the time domain. Overall, the complexity of frequency-domain UFMC TX processing as proposed in (Wild and Schaich, 2015) is 8 – 10 times the plain CP-OFDM processing complexity.

UFMC RX processing can be carried out by circularly overlapping and adding the $N_{\text{FILT}} - 1$ first and last samples of each received UFMC symbol and then taking the FFT of length N_{OFDM}. Therefore, the complexity of UFMC RX is the same as for plain

OFDM. Additionally, WOLA-type processing prior to overlap-and-add and FFT can be used for further reducing OOB emissions (Zayani et al., 2016).

UFMC preserves the orthogonality of the subcarriers in the absence of multipath channel. In addition, the channel estimation/equalization, PAPR reduction, and multiple-input multiple-output (MIMO) schemes developed for OFDM are applicable for UFMC. The drawback is that, for equalization, the TX filter coefficients have to be known by the RX. Due to the use of ZP, UFMC is not compatible with 5G NR baseline waveform, CP-OFDM. In addition, the prototype filter order is limited by the ZP length and when considering ZP lengths similar to CP lengths specified for 5G NR, the performance is quite poor in a mixed-numerology scenario, as illustrated in Section 3.

Filter-bank Multicarrier

Filtering at the subband level, as in the previously described schemes, involves filters of relatively short response (and hence of low complexity and latency) and is a compromise between whole-band and subcarrier-wise filtering. Filtering at the subcarrier level instead offers increased flexibility, facilitating per-subcarrier processing and tuning, at the cost of higher complexity and latency resulting from the use of longer filters. This makes FBMC most suitable for applications requiring finer granularity in spectrum sharing or narrow-band interference rejection capability, such as cognitive radio (Renfors et al., 2017). With its low OOB emission and high spectral efficiency and agility, FBMC is also well suited to uncoordinated multiple access (Tonello, 2003; Li et al., 2019) and heterogeneous networks (Renfors et al., 2017). Potential applications of FBMC include cognitive radio (PHYDYAS, nd), multimedia broadcasting (de la Fuente et al., 2016), mission-critical (EMPHATIC, nd), (Renfors et al., 2017, Chapter 3), machine-type (Li et al., 2019), optical (Renfors et al., 2017, Chapter 4), and, more recently, satellite communications (Kofidis and Dalakas, 2019), among others. Certain FBMC schemes have been considered as candidate 5G waveforms (Gerzaguet et al., 2017), (Renfors et al., 2017, Chapter 1) in view of their prominent merits compared with classical CP-OFDM and are briefly reviewed here.

An FBMC system can always be viewed as a transmultiplexer (TMUX) (Akansu et al., 1998), that is, a multirate FB system in its synthesis-analysis configuration, with modulation and demodulation being realized via a synthesis filter bank (SFB) and an analysis filter bank (AFB), respectively (Renfors et al., 2017, Chapter 5). Though not necessarily the case (e.g., (Chang, 1966)), most practical FBMC schemes employ modulated FBs, that is, subcarrier filters are frequency-shifted versions of a single prototype, facilitating both the design and the efficient implementation of the system (Renfors et al., 2017, Chapter 8). Overlapping of the transmitted pulses in both time and frequency is necessary to achieve high spectral efficiency (Chang, 1966). However, the overlap has to be small enough for the system to be robust to time and frequency dispersion, which asks for a time-frequency (TF) well-localized prototype filter. Moreover, the pulse shape has to be so designed as to satisfy the conditions for a (near) perfect reconstruction (PR) TMUX. Although a biorthogonal frequency-

division multiplexing (BFDM) system (with different TX and RX pulses) can be considered in general (Renfors et al., 2017, Chapter 1), practical waveforms almost always result from orthogonal systems, with a matched RX prototype filter, which maximizes the signal-to-noise ratio (SNR) and enhances compatibility among transceivers, at the cost of a somewhat longer delay (Renfors et al., 2017, Chapter 1). Nevertheless, the theory of TF analysis says that the following three requirements cannot be simultaneously met (Renfors et al., 2017, Chapter 7):

1) orthogonality in the complex domain,
2) maximum spectral efficiency (that of CP-free OFDM), and
3) best time-frequency localization (TFL) of the prototype filter.

Realizable FBMC schemes must therefore result from relaxing and trading off some of these requirements, at least to some extent.

Filter-bank multicarrier with offset-QAM (FBMC/OQAM) (Bellanger, 2010; Renfors et al., 2017), the historically first practical multicarrier modulation (MCM) solution for complex symbol transmission (Saltzberg, 1967; Hirosaki, 1981), satisfies (2) and (3) while relaxing (1) to orthogonality in the real domain only. This is done by splitting each quadrature amplitude modulation (QAM) symbol into its real (in-phase) and imaginary (quadrature) parts, with an offset of half symbol duration between them. Alternately offsetting real against imaginary parts and vice versa in both time and frequency can be shown to achieve real-domain orthogonality regardless of the prototype filter used (Fliege, 1992), provided that well-known (near) PR conditions (those for cosine-modulated (Tzannes et al., 1994; Farhang-Boroujeny and Yuen, 2010) or modified DFT (MDFT) (Fliege, 1992) FBs) are satisfied (Siohan et al., 2002). The degrees of freedom that result from the relaxation of (1) can be used to design prototype filters of optimum TFL (Renfors et al., 2017, Chapter 8). This in turn allows CP-free transmission and results in negligible frequency overlapping with non-adjacent subcarriers, thus supporting maximum spectral efficiency and increased robustness to time and frequency dispersion.

Channel equalization, however, may be more complicated than in CP-OFDM, especially for highly selective channels (Farhang-Boroujeny, 2011), (Renfors et al., 2017, Chapter 12). This is also due to the two-dimensional (in both time and frequency) self interference that the lack of complex-domain orthogonality intrinsically generates. Coping with the intrinsic interference in FBMC/OQAM can be a real challenge, in MIMO systems in particular (Pérez-Neira et al., 2016). Another consequence of the adoption of OQAM is that subcarrier-level processing is done at twice the symbol rate (Bellanger, 2010). Ways to mitigate these OQAM-induced complications are based on relaxing conditions (2) and/or (3) above, e.g., by utilizing CP or ZP (Cruz-Roldán et al., 2012). Alternatively, the so-called filter-bank multicarrier with QAM subcarrier modulation (FBMC/QAM) offers a compromise between CP-OFDM and FBMC/OQAM in terms of spectral confinement and spectral efficiency and can be realized in a number of ways. These include (i) inserting null symbols to restrict the intrinsic interference to the time or the frequency domain only (Zakaria and Le Ruyet, 2010), (ii) the employment of multiple FBs (with, for example, separate prototype fil-

ters for the even- and odd-indexed subcarriers) (Kim et al., 2016), and (iii) resorting to lapped orthogonal transforms of double size (Bellanger et al., 2015; Mattera et al., 2016).

An alternative way to reduce self interference, restricting it to the time domain only, is to again relax requirement (2) by sufficiently increasing the SCS so as to eliminate spectral overlapping among subcarriers (Vallet and Taieb, 1995). This, in effect, corresponds to oversampling (hence to a non-critically sampled TMUX) and gives rise to the so-called filtered multitone (FMT) scheme (Cherubini et al., 2002). Since emphasis is here put on the frequency localization of the subcarrier filters, inter-carrier interference (ICI) is completely avoided at the cost of the filters' time localization and length (and hence complexity and latency). Thus non-trivial per-subcarrier equalization to eliminate the ISI is still necessary in the baseline FMT employing no CP (Benvenuto et al., 2002). Alternatively, ISI can be dealt with in a concatenated CP-OFDM-FMT scheme (Tonello, 2006), which is very much reminiscent of the UFMC idea. FMT variants with controlled subcarrier overlapping and adjustable ICI are also possible (e.g., (Shao et al., 2017)). FMT has been considered for very high-speed digital subscriber line (VDSL) modems (Cherubini et al., 2000) and has been adopted in the TETRA enhanced data service (TEDS) standard for professional (or private) mobile radio (PMR) (Nouri et al., 2006).

Good time and/or frequency localization in the previous FBMC schemes is achieved at the expense of long tails for the prototype filters, which can be a factor of considerable spectral efficiency loss, especially in a sporadic (short burst) machine type communications (MTC) environment. To mitigate this drawback and meet the strict requirement of 5G networks for low latency, block FBMC versions have also become available, which resemble CP-OFDM. These block schemes sacrifice some of the spectral efficiency and confinement of FBMC in return for the advantages of CP-OFDM, which include easier equalization and efficient frequency-domain implementation. Grouping, in an FMT system, the symbols per subcarrier in blocks and using a periodically repeated version of the subcarrier filter, with a CP inserted per block, yields the so-called cyclic block-filtered multitone (CB-FMT) scheme (Girotto and Tonello, 2014). Without oversampling, the scheme known as generalized frequency-division multiplexing (GFDM) (Michailow et al., 2014) (Renfors et al., 2017, Chapter 1) results as a special case. Being non-orthogonal, it requires interference cancellation for demodulation at the receiver. Modifications aiming at enhancing its orthogonality include OQAM-based versions (Bandari et al., 2016; Matthé and Fettweis, 2016). When applied in an FBMC/OQAM system, the same ideas give rise to filter-bank multicarrier with circular offset-QAM (FBMC/COQAM) schemes (Abdoli et al., 2013; Lin and Siohan, 2014). Again, WOLA processing can be used to mitigate the effects of the discontinuity between consecutive blocks.

A common characteristic of all MCM schemes is their high PAPR, which can be particularly problematic with low-powered transmitters, such as user devices in the cellular UL (Renfors et al., 2017, Chapter 18). This problem can be addressed via single-carrier modulation (SCM) which, by exploiting the TF duality (Bingham, 2000, Section 5.4), generates single-carrier (SC)-like waveforms through a spread-

ing (precoding) of the input signal in the frequency domain. DFT precoding of CP-OFDM gives the DFT-s-OFDM scheme, which is an option for the UL of 5G NR and can also be seen as a special case of CB-FMT (Girotto and Tonello, 2017) and GFDM (Michailow et al., 2014). Filter-bank single-carrier (FB-SC) modulation results in an analogous manner from FBMC via DFT- or, more generally, FB-based precoding and enjoys the low PAPR property along with the advantages of FBMC over OFDM (Renfors et al., 2017, Chapter 7). A literature review of DFT-s-OFDM and FB-SC, with application in satellite communications, can be found in (Kofidis and Dalakas, 2019).

It should be noted that these and other FBMC schemes can be put in a so-called generalized (Gao et al., 2005; Kliks et al., 2011) or flexible (Gutiérrez et al., 2014; Lopez-Salcedo et al., 2013) modulation framework, whose importance in flexibly accommodating diverse use cases in future networks (Nissel et al., 2017) cannot be overestimated. FBMC research has been active, in spite of the adoption of enhanced OFDM in the air interface of 5G NR. In fact, more advanced MCM schemes like multicarrier (MC) faster-than-Nyquist (FTN) (Dasalukunte et al., 2011) and orthogonal time frequency space (OTFS) (Hadani et al., 2017) can be shown to have close connections with classical FBMC (e.g., (Lin et al., 2015; Nimr et al., 2018)).

Fast-Convolution Filter Bank

Fast-convolution filter bank (FC-FB) is an efficient way of realizing highly tunable multirate FB configurations (Renfors et al., 2014), (Renfors et al., 2017, Chapter 8). FC-FBs are based on FFT-IFFT pairs with overlapped block processing, and they offer a straightforward way to adjust the filters' frequency-domain characteristics, even in real time. Each subband can be easily configured for different bandwidths, center frequencies, and sampling rate conversion factors, including also partial or full-band near perfect reconstruction (NPR) systems. Such FB systems find various applications, for example, as flexible multichannel channelization filters for software defined radios (Renfors et al., 2017, Chapter 6). They have also the capability to implement simultaneous waveform processing for multiple single-carrier and/or multicarrier transmission channels with nonuniform bandwidths and subchannel spacings. The application of FC to multirate filters has been presented in (Princen, 1995; Muramatsu and Kiya, 1997; Borgerding, 2006), and FC implementations of channelization filters and FBs have been considered in (Boucheret et al., 1999; Zhang and Wang, 2000; Pucker, 2003; Umehira and Tanabe, 2010). The idea of FC implementation of NPR FB systems has been introduced in (Renfors and f. harris, 2011), and detailed analysis and FC-FB optimization methods are given in (Renfors et al., 2014).

In its basic form, FC implements convolution between two finite-length sequences $\mathbf{h}$ and $\mathbf{x}$ as follows:

$$\mathbf{y} = \mathbf{W}_L^{-1}\left[\left(\mathbf{W}_L\begin{bmatrix}\mathbf{h}\\ \mathbf{0}_{(L-L_h)\times 1}\end{bmatrix}\right)\odot\left(\mathbf{W}_L\begin{bmatrix}\mathbf{x}\\ \mathbf{0}_{(L-L_x)\times 1}\end{bmatrix}\right)\right]. \tag{1}$$

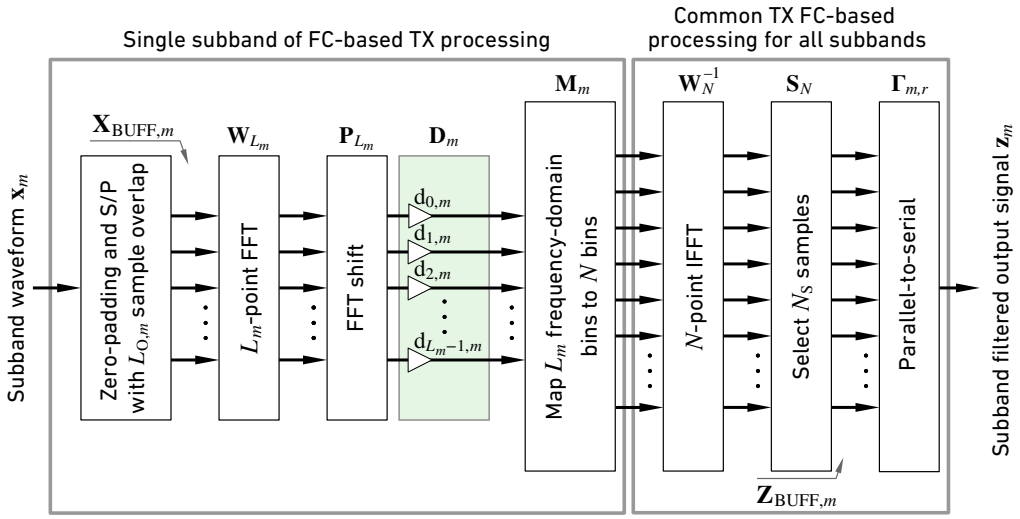

Figure 1: Fast-convolution-based flexible SFB using overlap-and-save processing. In this structure, the interpolation factor of subband m is equal to the ratio of the IFFT length N and the FFT length L_m. The number of overlapping input samples is $L_{\mathrm{O},m} = L_m - L_{\mathrm{S},m}$, where $L_{\mathrm{S},m}$ is the number of non-overlapping input samples.

Here, L_h and L_x are the lengths of $\mathbf{h}$ and $\mathbf{x}$, respectively, $\mathbf{W}_L$ and $\mathbf{W}_L^{-1}$ are DFT and inverse discrete Fourier transform (IDFT) matrices of size L, respectively, while $\mathbf{0}_{L\times 1}$ is the column vector of length L and $\odot$ denotes element-wise multiplication. This transform-domain processing implements circular (cyclic) convolution by nature, however, linear convolution is obtained if the transform length is high enough. The length of the linear convolution is $L_{\mathrm{LIN}} = L_h + L_x - 1$. The length L in (1) has to be at least L_{LIN}, otherwise circular distortion will appear in the result (Pelkowitz, 1981).

In order to process long sequences, block-wise FC with partly overlapping consecutive processing blocks can be used in conjunction with overlap-and-add (OLA) or overlap-and-save (OLS) processing (Stockham, Jr., 1966; Helms, 1967; Oppenheim and Schafer, 1989). In conventional OLS processing, the signal to be processed is first divided into blocks of length L such that each block overlaps with the previous block by L_{O} samples. Then these blocks are circularly convolved by the filter impulse response, L_{O} samples are discarded from the resulting output blocks, and the remaining parts are concatenated to form the output signal. Provided that L_{O} is greater than or equal to the order of the filter, the above processing evaluates the linear convolution exactly.

Fast-Convolution-based Synthesis Filter Bank

The structure of the FC-based adjustable SFB is illustrated in Fig. 1. The general idea of this structure is a multirate version of fast convolution (Borgerding, 2006; Boucheret et al., 1999). We consider the case where multiple low-rate narrowband signals $\mathbf{x}_m$

for $m = 0, 1, \ldots, M-1$ are to be filtered with adjustable frequency responses and possibly adjustable sampling rates and then combined into a single wideband signal $\mathbf{y}$, following the frequency-division multiplexing (FDM) principle. We are interested in the cases where the input signals are critically sampled or oversampled by a small factor. We also note that different subbands may be overlapping. The dual AFB structure of Fig. 1 can be used for splitting the incoming high-rate wideband signal into several low-rate narrowband signals.

In this structure, each of the M incoming signals is first zero-padded at the beginning and end by $S_{\mathrm{F},m} = L_m/2$ samples, where L_m is the forward transform (FFT) length in multirate FC processing. Let us denote these zero-padded signals by $\mathbf{x}_{\mathrm{ZP},m}$ for $m = 0, 1, \ldots, M-1$. The target of this zero padding is to preserve the first and last samples in OLS processing. These signals are then segmented into overlapping blocks of length L_m for $m = 0, 1, \ldots, M-1$ as follows:

$$[\mathbf{X}_{\mathrm{BUFF},m}]_{k,r} = [\mathbf{x}_{\mathrm{ZP},m}]_{rL_{\mathrm{S},m}+k} \tag{2}$$

for sample (row) indices $k = 0, 1, \ldots, L_m - 1$ and for FC block (column) indices $r = 0, 1, \ldots, R_m - 1$. The number of non-overlapping input samples is $L_{\mathrm{S},m}$ and the overlap factor in FC processing is determined as $\lambda = 1 - L_{\mathrm{S},m}/L_m$. The overlap factor of $\lambda = 1/2$ has turned out to be the most feasible value for compromising between the complexity and the performance as analyzed in (Yli-Kaakinen et al., 2017; Yli-Kaakinen et al., 2020). Now, the number of FC-processing blocks is given by $R_m = \lceil (2S_{\mathrm{F},m} + T_m - L_m)/L_{\mathrm{S},m} \rceil + 1$, where T_m is the length of $\mathbf{x}_m$. Each input block is then transformed to frequency domain using FFT of length L_m. The frequency-domain bin values of the converted signal are multiplied by the weight values of the frequency-domain window $\mathbf{d}_m$ consisting of ones on the passband, zeros on the stopband, and two symmetric transition bands with N_{TB} non-trivial optimized prototype transition-band weights (Yli-Kaakinen et al., 2017). Finally, the weighted signals are combined and converted back to time domain using IFFT of length N, and the resulting time-domain output blocks are concatenated using the OLS principle (Rabiner and Gold, 1975; Daher et al., 2010). The number of non-overlapping samples in OLS processing is $N_{\mathrm{S}} = N/L_m \times L_{\mathrm{S},m}$.

The FC processing can be represented using matrix formalism by decomposing the processing as the $N_{\mathrm{S}} \times L_m$ matrix

$$\mathbf{F}_m = \mathbf{S}_N \mathbf{W}_N^{-1} \mathbf{M}_m \mathbf{D}_m \mathbf{P}_{L_m} \mathbf{W}_{L_m}. \tag{3}$$

Here, $\mathbf{W}_{L_m}$ and $\mathbf{W}_N^{-1}$ are DFT and IDFT matrices of size L_m and N, respectively. The DFT shift matrix $\mathbf{P}_{L_m}$ is a permutation matrix swapping the upper and lower half-spaces while $\mathbf{D}_m = \mathrm{diag}(\mathbf{d}_m)$ is the diagonal matrix of size L_m with the frequency-domain weights of the subband m along the diagonal. The frequency-domain mapping matrix $\mathbf{M}_m \in \mathbb{N}^{N \times L_m}$ maps L_m frequency-domain bins of the input signal to L_m bins out of the total N bins $(c_m - \lceil L_m/2 \rceil + \ell \bmod N)$ for $\ell = 0, 1, \ldots, L_m - 1$, where c_m is the center bin of the subband m while $\mathbf{S}_N$ selects the desired N_{S} output samples from the inverse transformed signal corresponding to OLS processing.

The block-wise processing of signals can now be represented as

$$\mathbf{Z}_{\text{BUFF},m} = \mathbf{F}_m \mathbf{X}_{\text{BUFF},m}. \tag{4}$$

The high-rate subband waveform is obtained by concatenating processed blocks as given by

$$\mathbf{z}_m = \sum_{r=0}^{R_m-1} \Gamma_{m,r} [\mathbf{Z}_{\text{BUFF},m}]_r, \tag{5}$$

where

$$\Gamma_{m,r} = \begin{bmatrix} \mathbf{0}_{rN_\text{S} \times N_\text{S}} \\ \mathbf{I}_{N_\text{S}} \\ \mathbf{0}_{((R_m-1)N_\text{S}-rN_\text{S}) \times N_\text{S}} \end{bmatrix} \exp(\text{j}2\pi r \theta_m) \tag{6}$$

aligns the blocks to their desired locations and rotates the phases by $\theta_m = c_m L_{\text{S},m}/L_m$ for phase continuity. Here, $\mathbf{I}_{N_\text{S}}$ is the identity matrix of size N_S. In the basic FC-FB model, each subcarrier phase starts from zero in the beginning of each non-overlapping FC processing block. However, the non-overlapping block length corresponds to an integer number of subcarrier cycles only in special cases, and this effect has to be compensated by a constant phase rotation for each FC processing block. The needed phase rotation depends on the subcarrier center frequency and the non-overlapping block length in subcarrier samples. Finally, the overall waveform to be transmitted is obtained by summing all the M subband waveforms as

$$\mathbf{y} = \sum_{m=0}^{M-1} \mathbf{z}_m. \tag{7}$$

The multirate FC-processing of Fig. 1 increases the sampling rates of the subband signals by the factors

$$I_m = N/L_m = N_\text{S}/L_{\text{S},m}. \tag{8}$$

Given the IFFT length N, the sampling rate conversion factor is determined by the FFT length L_m, and it can be configured for each subband individually. Naturally, the FFT length determines the maximum number of nonzero frequency bins, i.e., the bandwidth of the subband. It is also possible to reduce the sampling rate conversion factor by increasing the FFT length by adding zero-valued bins outside the wanted subband frequency range.

In the above processing, the bandwidth of each subband can be easily tuned by adjusting the L_m frequency-domain weights in $\mathbf{D}_m$. Here, the maximum available bandwidth is determined by L_m. On the other hand, the center frequency of the subband can be adjusted by only cyclically shifting the columns of the frequency-domain mapping matrix $\mathbf{M}_m$ to their desired locations, while the interpolation factor is determined simply by the ratio of N and L_m. Therefore, this FC SFB provides an easily configurable basis for flexible multichannel channelization FB for flexible radio access schemes.

With FC-FB, it is easy to adjust the filtering bandwidth for the subbands individually. This is very useful in subband-filtered OFDM because there is no need to realize

filter transition bands and GBs between equally parameterized synchronous PRBs. In the extreme case, the group of filtered PRBs can cover the full carrier bandwidth, and FC filtering would implement tight channelization filtering for the whole carrier.

FC-FB as a Generic Waveform Processing Engine

The application of FC-FB in filtered-OFDM is discussed in more detail in Section 3. It can also be used for generating and detecting FBMC/OQAM and FMT-type multicarrier waveforms (Shao et al., 2015), as well as traditional Nyquist pulse shaping-based SC waveforms (Yli-Kaakinen and Renfors, 2015; Zhao et al., 2015). FC-FB can also be used for channelization filtering with arbitrary waveforms. Basically, the same processing structure, but without overlap processing, can be also used for implementing circular multicarrier waveforms, like GFDM, CB-FMT, and FBMC/COQAM.

As explained in (Renfors and Yli-Kaakinen, 2014), channel equalization for FBMC and FB-SC waveforms can thus be realized in a unified manner by combining the channel equalization weights with the (sub)channel weight masks in the FFT domain. Also synchronization-related functions can be effectively combined with the FC-FB processing structure, as discussed in (Renfors and Yli-Kaakinen, 2013).

Enhanced OFDM for 5G New Radio

Fifth-Generation Mixed Numerology

CP-OFDM has been selected as the baseline waveform for 5G NR at below 52.6 GHz frequency bands, while DFT-s-OFDM (also known as single-carrier frequency-division multiple access (SC-FDMA)) can also be used for UL in coverage-limited scenarios. 5G NR provides scalable numerology and frame structure in order to support diverse services, deployment scenarios, and user requirements operating from bands below 1 GHz to bands above 30 GHz known as millimeter-wave (mmWave). This numerology supports multiple SCSs in order to reduce latency and to provide increased robustness to phase noise and Doppler, especially at higher carrier frequencies. In addition, by increasing the SCS, the maximum channel bandwidth supported for a given OFDM transform length can be increased. On the other hand, smaller SCSs have the benefit of providing longer CP durations in time and, consequently, better tolerance to delay spread with reasonable overhead (Dahlman et al., 2018).

Three primary services provided by 5G NR are enhanced mobile broadband (eMBB), ultra-reliable low-latency communications (URLLC), and massive machine-type communications (mMTC). eMBB use cases include high-definition video streaming and virtual reality and, therefore, high throughput and low latency are essential requirements for providing high quality of experience for the end user. mMTC focuses on internet of things (IoT) applications where a massive number of devices transmit and receive small amount of data at low data rates. In mMTC, low power consumption is crucial. In contrast, URLLC is characterized by very high reliability

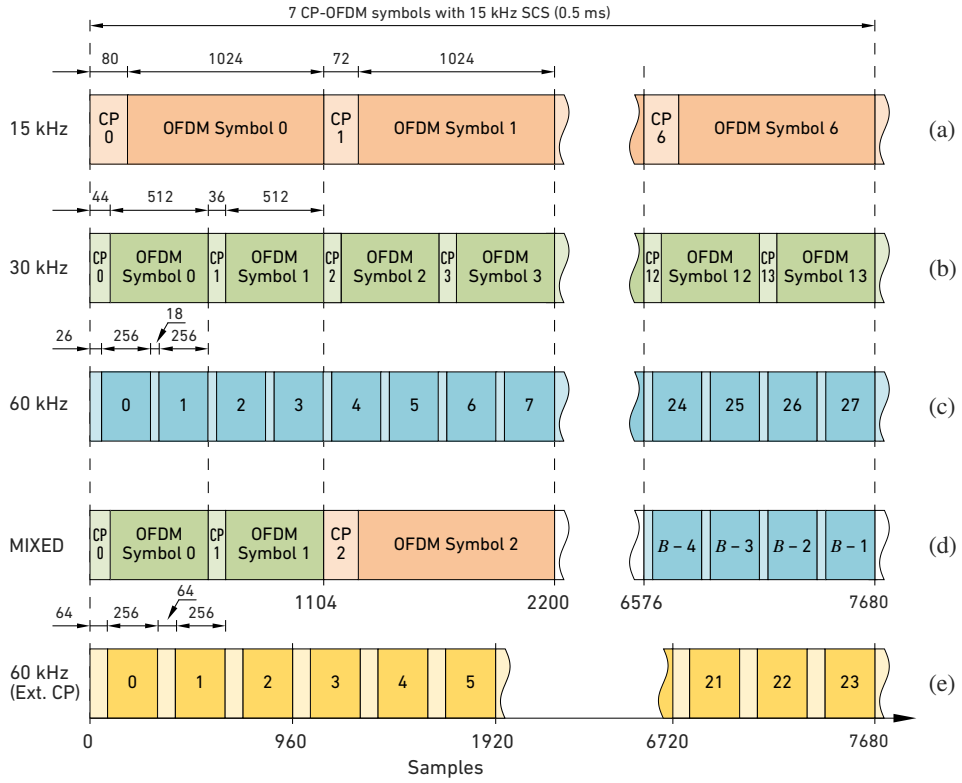

Figure 2: Illustration of multiple numerologies in the 10 MHz channel and their synchronization within the half subframe (0.5 ms). (a)–(c) 15 kHz, 30 kHz, and 60 kHz SCS with normal CP, respectively. (d) Time-multiplexed mixed numerology case. (e) 60 kHz SCS with extended CP.

and extremely low latency since the use cases focus on mission-critical applications, e.g., an industry automation and autonomous vehicles.

Similar to LTE technology, a radio frame of 10 ms is divided into 10 subframes, each having 1 ms duration whereas each subframe can have 2^{η} slots, where $\eta = 0, 1, \ldots, 5$. Each slot consists of either 14 or 12 OFDM symbols for the normal CP or extended CP, respectively (3GPP, 2019b; Dahlman et al., 2018). The slot length varies based on the SCS and the number of slots per subframe. As shown in Table 1, it is 1 ms for 15 kHz, 0.5 ms for 30 kHz and so on. SCS of 15 kHz occupies one slot per subframe, SCS of 30 kHz occupies two slots per subframe, and so on.

5G NR supports also non-slot based scheduling (so-called mini slots), where the transmission length can be configured between 1 and 13 symbols (3GPP, 2019a). This mini-slot concept is especially essential for low-latency URLLC and for dynamic TDD. Such transmissions can pre-empt the ongoing slot-based transmission and, therefore, also the time-domain flexibility of the processing solutions becomes crucial in the 5G NR context.

Fig. 2 shows the time alignment of different numerologies within a half subframe corresponding to a duration of 0.5 ms. In general, 5G NR does not specify the minimum number of consecutive symbols of certain SCS and, therefore, in extreme time-

Table 1: 5G NR mixed numerology in frequency range 1 (FR1).

Subcarrier spacing	15 kHz	30 kHz	60 kHz	$2^{\eta} \times 15$ kHz
OFDM symbol duration	66.7 µs	33.3 µs	16.7 µs	$2^{-\eta} \times 66.7$ µs
CP duration	4.69 µs	2.34 µs	1.17 µs	$2^{-\eta} \times 4.69$ µs
Number of OFDM symbols per slot	14	14	12 or 14	12 or 14
Slot duration	1000 µs	500 µs	250 µs	$2^{-\eta} \times 1000$ µs

multiplexing cases, it is possible that the SCS changes even at the symbol level as illustrated in Fig. 2(d).

5G NR allows the use of a mixed numerology, i.e., using different SCSs in different subbands (or bandwidth parts (BWPs) in the 5G NR terminology) within a single carrier. However, the use of different SCSs within an OFDM multiplex harms the orthogonality of subcarriers, introducing inter-numerology interference (INI) as explained in Section 3. To cope with INI in mixed-numerology scenarios with basic CP-OFDM, relatively wide GBs should be applied between adjacent BWPs, which would reduce the spectral efficiency. Alternatively, the 3rd generation partnership project (3GPP) allows to use spectrum enhancement techniques for CP-OFDM, but this should be done in a transparent way and without performance loss with respect to plain CP-OFDM. The transparency means that a TX or a RX does not need to know whether spectrum enhancement is used at the other end. The spectrum enhancement techniques should also be compatible with each other, allowing different techniques to be used in the TX and RX. Transparent enhanced CP-OFDM techniques have been considered in (Bazzi et al., 2017; Zayani et al., 2018; Levanen et al., 2019).

The main waveforms used in 5G NR are plain CP-OFDM, CP-OFDM with WOLA processing, and F-OFDM. These waveforms are mainly considered for below 6 GHz frequency bands where the channel bandwidths are narrower and the spectral resources are more limited compared to higher frequencies. WOLA and F-OFDM waveforms can be designed to ensure the backward compatibility with legacy OFDM, that is, enhanced CP-OFDM waveforms can be received with plain CP-OFDM RX or, alternatively, the plain CP-OFDM waveform can be received with enhanced CP-OFDM RX.

Windowed Overlap-Add

WOLA is a low-complexity scheme where the transitions between CP-OFDM symbols are windowed by smooth functions (typically raised cosine (RC) window) to reduce the spectral leakage of the TX waveform and to improve the selectivity of the RX processing. Generally, the spectrum control capability of WOLA is limited by the length of the cyclic extensions between OFDM symbols. For effective spectrum control, the cyclic extension length should be increased beyond the CP lengths used in LTE or 5G NR numerologies, thus reducing the spectral efficiency.

In WOLA TX processing, the CP-OFDM symbols to be transmitted are cyclically extended on both ends by N_{EXT} samples and then the extended symbols are win-

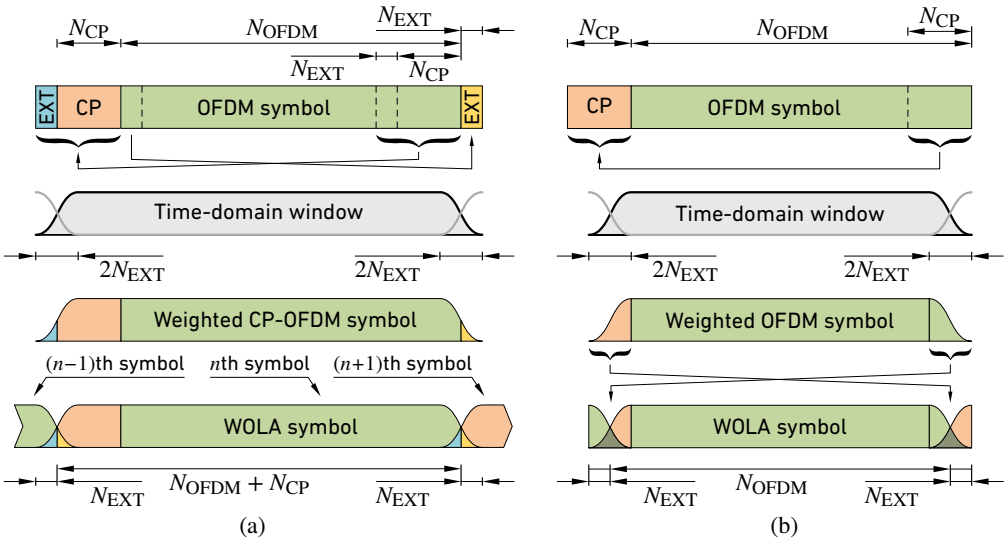

Figure 3: Windowed overlap-and-add (WOLA) (a) TX and (b) RX processing.

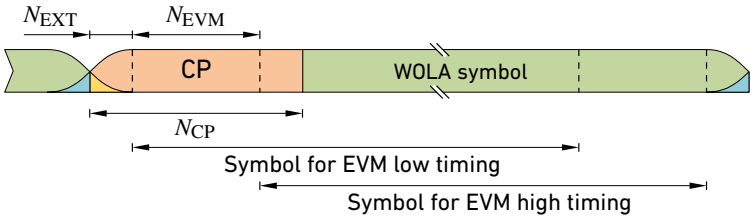

Figure 4: Windowed overlap-and-add (WOLA) TX processing for an EVM window of N_{EVM} samples.

dowed by amplitude-complementary window function where both the raising and falling edges of the window are of $2N_{EXT}$ samples, as illustrated in Fig. 3(a). The overall window length in WOLA TX processing is $N_{CP} + N_{OFDM} + 2N_{EXT}$, where N_{OFDM} and N_{CP} are the OFDM symbol and CP lengths, respectively. Finally, the windowed consecutive symbols are overlapped and added such that the overlap between each pair of symbols is $2N_{EXT}$ samples. In WOLA RX processing, the window length is only $N_{OFDM} + 2N_{EXT}$ and the windowed parts of each symbol are circularly overlapped and added as depicted in Fig. 3(b). In order to prevent the contamination of the payload data within the symbol, the WOLA TX processing extension should be selected to be $N_{EXT} = (N_{CP} - N_{EVM})/2$, where N_{EVM} is the EVM window length used for characterizing the EVM degradation with respect to timing errors (3GPP, 2019b). The EVM window and the corresponding EVM measurement timing instances before and after the middle of the CP are illustrated in Fig. 4.

Time-Domain Filtered OFDM

For time-domain F-OFDM, a Hann-windowed sinc impulse response, as given by

$$h(n) = \sqrt{\frac{1}{2}\left(1 + \cos\left(\frac{2\pi n}{N_{\text{FILT}} - 1}\right)\right)}\,\text{sinc}\left(\frac{n(L_{\text{ACT}} + L_{\text{EBW}})}{N_{\text{OFDM}}}\right), \tag{9}$$

for $n = -N_{\text{FILT}}/2, -N_{\text{FILT}}/2+1, \ldots, N_{\text{FILT}}/2$, was originally proposed in (Zhang et al., 2015). The passband of the filter is adjusted to span over the L_{ACT} active subcarriers as well as the excess bandwidth determined in number of subcarriers by L_{EBW} in order to prevent the degradation of edge subcarriers. The filter order is selected to be half of the symbol length as $N_{\text{FILT}} = N_{\text{OFDM}}/2$ and, therefore, the complexity of the filtering, in terms of real multiplications, is $C_{\text{F-OFDM}} = 2(N_{\text{OFDM}}/2 + 1)(N_{\text{OFDM}} + N_{\text{CP}})$ per CP-OFDM symbol. Here it is assumed that the coefficient symmetry is utilized for the filter and that the F-OFDM waveform is generated and filtered on the baseband with real-valued filter impulse response.

The analytical expression for the filter coefficient values in (9) enables simple adjustment of the filter bandwidth based on the bandwidth needed for the allocated subcarriers. However, the excessive complexity limits the applicability of the time-domain F-OFDM. The complexity can be reduced by using the approach based on polyphase FB structures (Tonello, 2006; Zakaria and Le Ruyet, 2012; Li et al., 2014; Zayani et al., 2018). However, in this case the subbands typically have the same bandwidths and, therefore, the configurability is highly impaired.

Fast-Convolution Filtered OFDM

To generate the FC filtered OFDM waveform, the FC-FB of Section 3 is applied for subband-level filtering while utilizing normal CP-OFDM waveform for the group of PRBs (Renfors et al., 2015, 2016; Yli-Kaakinen et al., 2017). One application is in cellular UL scenarios, in which the different user equipments (UEs) utilize different groups of PRBs for their transmissions. UEs may utilize single-subband FC filtering or the corresponding time-domain filtering to shape their spectra. For good isolation of different users' subbands, a few subcarriers are needed as GBs between the subbands. Good OOB emission characteristics allow us to relax the tight synchronization requirements of traditional uplink orthogonal frequency-division multiple access (OFDMA). On the base-station side, an FC-based AFB is used for separating the subbands of different UEs. Furthermore, it becomes possible to parameterize the waveforms differently for different UEs, e.g., using different SCSs, CP lengths, and/or frame structures (Renfors et al., 2016). Anyway, synchronous UEs with common numerology can also be operated within a single subband. Concerning cellular downlink (DL) scenarios, synchronization is not an issue, but the filtered OFDM idea would still make it possible to parameterize individually different users' signals in different BWPs.

FC-FB Performance in the 5G Context

As an example, let us consider the channelization of two 5 MHz BWPs within the 10 MHz channel. The SCSs of the BWPs are $f_{\text{SCS},0} = 15$ kHz and $f_{\text{SCS},1} = 30$ kHz and the GB between the BWPs is 180 kHz. The numbers of active PRBs for BWPs with 15 kHz and 30 kHz SCS are $N_{\text{PRB},0} = 26$ and $N_{\text{PRB},1} = 13$ ($L_{\text{ACT},0} = 312$ and $L_{\text{ACT},1} = 156$), respectively, while the numbers of OFDM symbols are $B_{\text{OFDM},0} = 14$ and $B_{\text{OFDM},1} = 28$, respectively. The CP lengths for the BWPs are selected as illustrated in Fig. 2. The required IFFT transform lengths for OFDM modulation are $N_{\text{OFDM},0} = 1024$ and $N_{\text{OFDM},1} = 512$. Assuming that the split-radix IFFT is used for evaluating the IFFTs, their complexities, in terms of real multiplications, are $C_{\text{IFFT},0} = 7172$ and $C_{\text{IFFT},1} = 3076$. Therefore, the overall number of real multiplications needed for processing both BWPs for plain CP-OFDM TX is $C_{\text{OFDM}} = 186\,536$.

For WOLA processing, the cyclic extensions for the first and second BWP are $N_{\text{EXT},0} = 36$ and $N_{\text{EXT},1} = 18$, respectively, and the complexity for WOLA TX processing (excluding the OFDM modulation) is only $C_{\text{WOLA}} = 8064$ real multiplications. Here, we assume that the window weights are real-valued and that two real multiplications are needed for real-by-complex multiplications. It is pointed out that, when using the EVM evaluation as specified in (3GPP, 2019b), shorter cyclic extensions have to be used due to the EVM windows used in the evaluation. For time-domain F-OFDM processing, the filter length is assumed to be half of the symbol length and the number of samples for each BWP is 15 360, therefore, the number of real multiplications needed for time-domain filtering is $C_{\text{F-OFDM},0} = 8.67 \times 10^6$ and $C_{\text{F-OFDM},1} = 4.28 \times 10^6$ for the first and the second BWP, respectively. In addition, 125 952 multiplications are needed for modulating the BWPs to the desired frequency. Overall, these figures can be reduced to some extent by first carrying out the OFDM modulation using smaller transforms (at lower sample rate) and then interpolating the low-rate CP-OFDM waveform to the final output rate using polyphase interpolator.

The FC-processing complexity consists of forward (FFT) and inverse (IFFT) transforms as well as of frequency-domain windowing. The OFDM IFFT transform sizes on the low-rate side can be selected, e.g., as the smallest power-of-two values covering the active subcarriers and two transition bands, as expressed in

$$L_{\text{OFDM},m} = 2^{\lceil \log_2 (L_{\text{ACT},m} + 2N_{\text{TB}}) \rceil} \tag{10}$$

for $m = 0, 1$ while the FC-processing short and long transform lengths are selected as

$$\frac{N}{L_m} = \frac{N_{\text{OFDM},m}}{L_{\text{OFDM},m}} \tag{11}$$

for $m = 0, 1$. In this case, FC SFB processing interpolates the CP-OFDM waveform to the desired sample rate. For the given number of active subcarriers, the IFFT transform lengths for OFDM modulation are selected as $L_{\text{OFDM},0} = 512$ and $L_{\text{OFDM},1} = 256$. The FC-processing FFT and IFFT transform lengths are $N = 2L_0 = 2L_1 = 1024$, that is, the FC processing interpolates the CP-OFDM waveforms by a factor of two resulting in OFDM symbol lengths of $N_{\text{OFDM},0} = 2L_{\text{OFDM},0} = 1024$

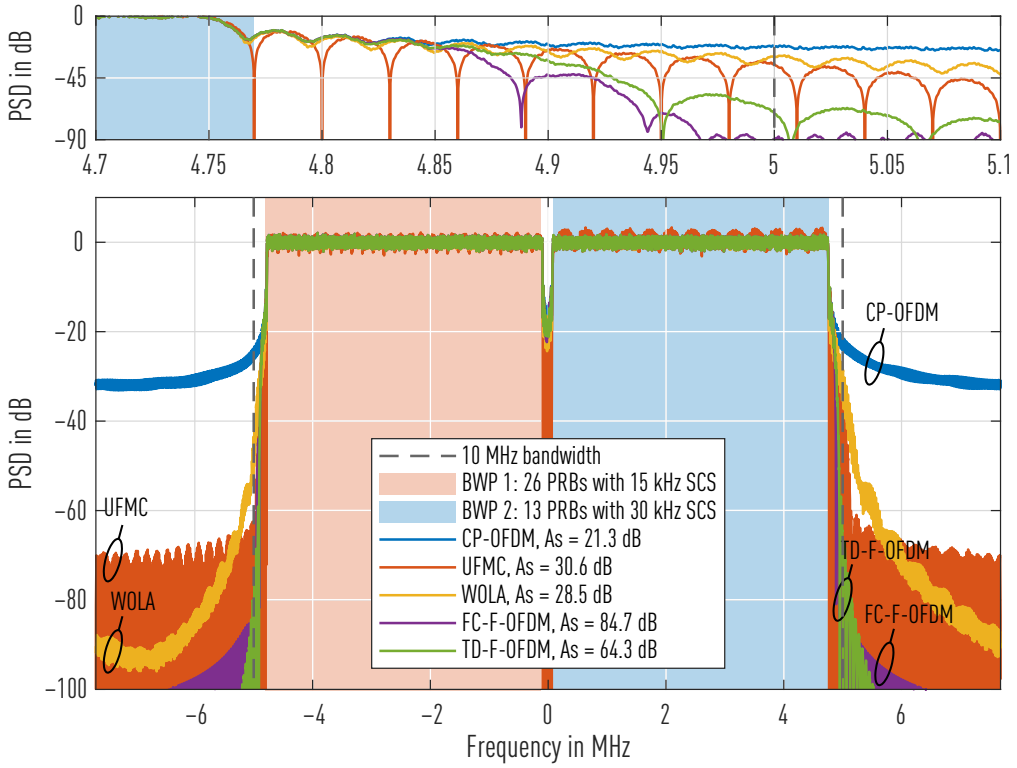

Figure 5: Channelization of two BWPs with 15 kHz and 30 kHz subcarrier spacing (SCS) within a 10 MHz channel. The lower subfigure shows the overall responses while the upper subfigure shows the transition-band details. The minimum attenuation at channel edge, A_s, is given for each waveform.

and $N_{\text{OFDM},1} = 2L_{\text{OFDM},1} = 512$. The FFTs and windowing need to be carried out subband-wise for $R_0 = R_1 = 32$ processing blocks whereas the IFFTs for the two BWPs can be combined. Here, $N_{\text{TB}} = 12$ real-valued transition-band weights are used for constructing the frequency-domain window and the overall complexity for FC processing with a given parameterization is only $C_{\text{FC-OFDM}} = 416\,020$ real multiplications.

It should be noted that the UFMC with PRB-wise filtering can also be conveniently realized using the FC-processing scheme described in Section 3. In this case, IFFT transform lengths for OFDM modulation are selected as $L_{\text{OFDM},m} = 64$ for $m = 0, 1, \ldots, N_{\text{PRB},0} - 1$ and $L_{\text{OFDM},m} = 32$ for $m = N_{\text{PRB},0}, N_{\text{PRB},0} + 1, \ldots, N_{\text{PRB},0} + N_{\text{PRB},1} - 1$ while the FFT and IFFT transform lengths are $N = 16L_m = 128$, that is, now the interpolation factor in FC processing is 16 resulting to OFDM symbol lengths of $N_{\text{OFDM},m} = 16L_{\text{OFDM},m} = 1024$ for $m = 0, 1, \ldots, N_{\text{PRB},0} - 1$ and $N_{\text{OFDM},m} = 16L_{\text{OFDM},m} = 512$ for $m = N_{\text{PRB},0}, N_{\text{PRB},0}+1, \ldots, N_{\text{PRB},0}+N_{\text{PRB},1}-1$. In this case, the overall complexity is $C_{\text{FC-UFDM}} = 840\,032$ real multiplications. However, the discontinuous symbol-synchronized FC processing as proposed in (Yli-Kaakinen et al., 2018) has to be utilized due to the non-integer ZP lengths for OFDM transform lengths smaller than 128.

Table 2: In-band mean-squared error (MSE) performance with various TX/RX processing pairs.

	BWP	CP-OFDM RX	WOLA RX	FC-F-OFDM RX	TD-F-OFDM RX
CP-OFDM TX	1	−30.1 dB	−33.1 dB	−33.0 dB	−33.0 dB
	2	−30.0 dB	−44.0 dB	−44.5 dB	−44.9 dB
WOLA TX	1	−33.0 dB	−43.4 dB	−47.0 dB	−47.0 dB
	2	−30.5 dB	−41.4 dB	−50.0 dB	−49.8 dB
FC-F-OFDM TX	1	−33.0 dB	−54.7 dB	−51.8 dB	−51.6 dB
	2	−29.9 dB	−42.8 dB	−45.0 dB	−45.0 dB
TD-F-OFDM TX	1	−33.1 dB	−54.9 dB	−51.8 dB	−51.6 dB
	2	−29.9 dB	−42.6 dB	−45.0 dB	−44.6 dB

Table 3: Complexity of 5G NR TX processing alternatives. Here, $C_{\text{TX}}/C_{\text{CP-OFDM}}$ denotes the TX complexity with respect to plain CP-OFDM TX.

	OFDM IFFT	Filtering	Total	$\mathbf{C_{TX}/C_{CP\text{-}OFDM}}$
CP-OFDM	186 536	0	186 536	1.00
WOLA	186 536	8064	188 888	1.04
TD-F-OFDM	186 536	13.1×10^6	13.3×10^6	71.13
FC-F-OFDM	79 016	416 020	495 036	2.65

The power spectral density (PSD) estimates for the processing alternatives are shown in Fig. 5 while the in-band MSE performance of TX/RX alternatives is given in Table 2. The PSD for UFMC is also shown here for reference. In this case, the prototype filter lengths for UFMC are $N_{\text{FILT},0} = 87$ and $N_{\text{FILT},1} = 49$ for BWPs with 15 kHz SCS and 30 kHz SCS, respectively. As seen from Fig. 5, FC-filtered-OFDM has clearly the lowest OOB emissions at channel edge whereas the best MSE performance is obtained using either time- or frequency-domain filtered OFDM. The complexity comparison, shown in Table 3, suggests that the complexity of FC-filtered-OFDM is only 2.65 times that of the plain CP-OFDM and 3.73 % that of the time-domain filtered OFDM.

In WOLA TX, the overlap-and-add processing of the nth symbol can not be carried out until the $(n+1)$st symbol has been windowed, as illustrated in Fig. 3(a). Therefore, the latency of WOLA processing is one symbol period. For linear-phase time-domain digital filters, the delay in samples is typically determined as half of the filter order and assuming that the filter order is half the symbol length, the resulting delay is one quarter of the symbol period. For a FC-based filter, the latency is given as $\tau = I_m S_{\text{F},m}$, where I_m is the interpolation factor, as given by (8), and $S_{\text{F},m}$ is the zero padding used in the processing, that is, for a typical value of $S_{\text{F},m} = L_m/2$, the latency is one symbol duration. However, the FC-processing latency can be reduced by using the generalized FC processing as proposed in (Yli-Kaakinen et al., 2020).

A Matlab/Octave model illustrating the above CP-OFDM-based processing alternatives can be downloaded from https://yli-kaakinen.fi/wp/filtered-multicarrier-transmission/.

Concluding Remarks

This chapter has focused on the spectral properties of filtered multicarrier transmission schemes, including the family of FBMC waveforms and different variants of enhanced OFDM. FBMC with offset-QAM subcarrier modulation enjoys the properties of best time-frequency localization and maximum spectral efficiency, at the cost of compromising the orthogonality of subcarriers in the complex domain. Thus, it suffers from inconveniences due to the OQAM signal structure, e.g., in the context of certain multi-antenna transmission schemes. Various alternatives exist for FBMC transmission using complex QAM, however at the expense of somewhat reduced spectral efficiency or orthogonality. FBMC schemes in general also suffer from higher complexity and latency, which makes them less appropriate than enhanced OFDM to meet the 5G NR needs.

3GPP chose CP-OFDM as the baseline waveform for the 5G NR at below 52.6 GHz frequency bands. Additional signal processing can be used on the TX side to reduce OOB emissions and on the RX side to suppress OOB interferences. However, the spectrum enhancement scheme adopted should be transparent and capable of operating without performance loss when plain OFDM processing is applied at the other end of the transmission link. The time-domain windowing-based WOLA scheme is widely considered as a low-complexity solution for spectrum enhancement at both ends. However, its capability of sidelobe suppression is rather limited with the CP lengths adopted for 5G NR. Subband-wise filtering of OFDM (F-OFDM) is more effective, but requires balancing between in-band interference and spectral efficiency loss due to GBs between BWPs. FFT-domain filtering based on the FC approach was found to be a highly flexible and efficient way to implement filtered OFDM.

Considering the high PAPR of OFDM signals, DFT-precoded OFDM (also known as DFT-s-OFDM) can be a better option for UL transmission due to its greatly reduced PAPR. The WOLA and F-OFDM schemes are directly applicable also for spectrum enhancement of these low-PAPR waveforms.

Bibliography

3GPP (2019a). *5G; Study on New Radio (NR) Access Technology (Release 15)*. document TR 38.912 V15.0.0.

3GPP (2019b). *Technical Specification Group Radio Access Network; NR; Base Station (BS) Radio Transmission and Reception (Release 15)*. document TS 38.104 V16.0.0.

Abdoli, J., Jia, M., and Ma, J. (2013). Weighted circularly convolved filtering in OFDM/OQAM. In *Proc. IEEE Int. Symp. Personal, Indoor, Mobile Radio Commun. (PIMRC)*, pages 657–661, London, UK.

Akansu, A. N., Duhamel, P., Lin, X., and de Courville, M. (1998). Orthogonal transmultiplexers in communication: A review. *IEEE Trans. Signal Process.*, 46(4):979–995.

Bala, E., Li, J., and Yang, R. (2013). Shaping spectral leakage: A novel low-complexity transceiver architecture for cognitive radio. *IEEE Veh. Technol. Mag.*, 8(3):38–46.

Bandari, S. K., Mani, V. V., and Drosopoulos, A. (2016). OQAM implementation of GFDM. In *Proc. IEEE Int. Conf. Telecommun. (ICT)*, Thessaloniki, Greece.

Banelli, P., Buzzi, S., Colavolpe, G., Modenini, A., Rusek, F., and Ugolini, A. (2014). Modulation formats and waveforms for 5G networks: Who will be the heir of OFDM? *IEEE Signal Process. Mag.*, pages 80–93.

Bazzi, J., Kusume, K., Weitkemper, P., Takeda, K., and Benjebbour, A. (2017). Transparent spectral confinement approach for 5G. In *Proc. European Conf. Networks Commun. (EuCNC)*, pages 1–5, Oulu, Finland.

Beaulieu, N. C. and Tan, P. (2007). On the effects of receiver windowing on OFDM performance in the presence of carrier frequency offset. *IEEE Trans. Wireless Commun.*, 6(1):202–209.

Bellanger, M. (2010). FBMC physical layer: A primer. Technical report, PHYDYAS project.

Bellanger, M., Mattera, D., and Tanda, M. (2015). Lapped-OFDM as an alternative to CP-OFDM for 5G asynchronous access and cognitive radio. In *Proc. IEEE Veh. Techn. Conf. (VTC Spring)*, Glasgow, UK.

Benvenuto, N., Tomasin, N., and Tomba, L. (2002). Equalization methods in OFDM and FMT systems for broadband wireless communications. *IEEE Trans. Commun.*, 50(9):1413–1418.

Bingham, J. A. C. (2000). *ADSL, VDSL, and Multicarrier Modulation*. John Wiley & Sons, Inc.

Borgerding, M. (2006). Turning overlap-save into a multiband mixing, downsampling filter bank. *IEEE Signal Process. Mag.*, pages 158–162.

Boucheret, M.-L., Mortensen, I., and Favaro, H. (1999). Fast convolution filter banks for satellite payloads with on-board processing. *IEEE J. Sel. Areas Commun.*, 17(2):238–248.

Brandes, S., Cosovic, I., and Schnell, M. (2006). Reduction of out-of-band radiation in OFDM systems by insertion of cancellation carriers. *IEEE Commun. Lett.*, 10(6):420–422.

Chang, R. W. (1966). Synthesis of band-limited orthogonal signals for multi-channel data transmission. *Bell. Syst. Tech. J.*, 45:1775–1796.

Chen, H., Chen, W., and Chung, C. (2011). Spectrally precoded OFDM and OFDMA with cyclic prefix and unconstrained guard ratios. *IEEE Trans. Wireless Commun.*, 10(5):1416–1427.

Chen, H., Hua, J., Li, F., Chen, F., and Wang, D. (2019). Interference analysis in the asynchronous f-OFDM systems. *IEEE Trans. Commun.*, 67(5):3580–3596.

Cherubini, G., Eleftheriou, E., and Ölçer, S. (2002). Filtered multitone modulation for very high-speed digital subscriber lines. *IEEE J. Sel. Areas Commun.*, 20(2):1016–1028.

Cherubini, G., Eleftheriou, E., Ölçer, S., and Cioffi, J. M. (2000). Filter bank modulation techniques for very high-speed digital subscriber lines. *IEEE Commun. Mag.*, pages 98–104.

Cosovic, I., Brandes, S., and Schnell, M. (2006). Subcarrier weighting: A method for sidelobe suppression in OFDM systems. *IEEE Commun. Lett.*, 10(6):444–446.

Cruz-Roldán, F., Blanco-Velasco, M., and Llorente, J. I. G. (2012). Zero-padding or cyclic prefix for MDFT-based filter bank multicarrier communications. *Signal Processing*, 92:1646–1657.

Daher, A., Baghious, E.-H., Burel, G., and Radoi, E. (2010). Overlap-save and overlap-add filters: Optimal design and comparison. *IEEE Trans. Signal Process.*, 58(6):3066–3075.

Dahlman, E., Parkvall, S., and Sköld, J. (2018). *5G NR: The Next Generation Wireless Access Technology*. Academic Press.

Dai, G., Chen, S., and Wang, G. (2019). Orthogonal projection with optimized reserved subcarriers mapping for sidelobe suppression in OFDM systems. *IEEE Access*, 7:29662–29671.

Dasalukunte, D., Rusek, F., and Öwall, V. (2011). Multicarrier faster-than-Nyquist transceivers: Hardware architecture and performance analysis. *IEEE Trans. Circuits Syst. I*, 58(4):827–838.

de la Fuente, A., Pérez Leal, R., and Garcia Armada, A. (2016). New technologies and trends for next generation mobile broadcasting services. *IEEE Commun. Mag.*, 54(11):217–223.

EMPHATIC (n.d.). Enhanced multicarrier techniques for professional ad-hoc and cell-cased communications. Technical report, FP7-ICT Project 318362 EMPhAtiC.

Farhang-Boroujeny, B. (2011). OFDM versus filter bank multicarrier. *IEEE Signal Process. Mag.*, 28(3):92–112.

Farhang-Boroujeny, B. and Yuen, C. H. (2010). Cosine modulated and offset QAM filter bank multicarrier techniques: A continuous-time prospect. *EURASIP J. Advances in Signal Processing*, 2010(8):1–16.

Faulkner, M. (2000). The effect of filtering on the performance of OFDM systems. *IEEE Trans. Veh. Technol.*, 49(9):1877–1884.

Fliege, N. J. (1992). Orthogonal multiple carrier data transmission. *Eur. Trans. Telecommun.*, 3(3):255–264.

Gao, X., You, X., Jiang, B., Pan, Z., and Wang, X. (2005). Generalized multi-carrier transmission technique for B3G mobile communications. *China Commun.*, pages 55–61.

Gerzaguet, R., Bartzoudis, N., Leonardo Gomes Baltar, V. B., Doré, J.-B., Kténas, D., Font-Bach, O., Mestre, X., Payaró, M., Färber, M., and Roth, K. (2017). The 5G candidate waveform race: A comparison of complexity and performance. *EURASIP J. Advances in Signal Processing*, 2017(13).

Girotto, M. and Tonello, A. M. (2014). Orthogonal design of cyclic block filtered multitone modulation. In *Proc. European Wireless Conf. (EW)*, Barcelona, Spain.

Girotto, M. and Tonello, A. M. (2017). Adaptive zero padded CB-FMT for LTE uplink transmission in the high mobility scenario. In *Proc. EURASIP European Signal Process. Conf. (EUSIPCO)*, Kos island, Greece.

Gutiérrez, E., López-Salcedo, J. A., and Seco-Granados, G. (2014). Systematic design of transmitter and receiver architectures for flexible filter bank multi-carrier signals. *EURASIP J. Advances in Signal Processing*, 2014(103):1–26.

Hadani, R., Rakib, S., Tsatsanis, M., Monk, A., Goldsmith, A. J., Molisch, A. F., and Calderbank, R. (2017). Orthogonal time frequency space modulation. In *Proc. IEEE Wireless Commun. Netw. Conf. (WCNC)*, San Francisco, CA, USA.

Helms, H. D. (1967). Fast Fourier transform method of computing difference equations and simulating filters. *IEEE Trans. Audio Electroacoust.*, AU-15(2):85–90.

Hirosaki, B. (1981). An orthogonally multiplexed QAM system using the discrete Fourier transform. *IEEE Trans. Commun.*, 29(7):982–989.

Kim, C., Yun, Y. H., Kim, K., and Seol, J.-Y. (2016). Introduction to QAM-FBMC: From waveform optimization to system design. *IEEE Commun. Mag.*, pages 66–73.

Kliks, A., Stupia, I., Lottici, V., Giannetti, F., and Bader, F. (2011). Generalized multi-carrier: An efficient platform for cognitive wireless applications. In *Proc. IEEE Int. Workshop on Multi-Carrier Systems & Solutions (MC-SS)*, Herrsching, Germany.

Kofidis, E. and Dalakas, V. (2019). Filter bank-based multicarrier modulation for multiple access in next generation satellite uplinks: A DVB-RCS2-based experimental study. In *Proc. IEEE 5G World Forum (5GWF)*, Dresden, Germany. Workshop on Satellite and Non-Terrestrial Networks for 5G.

Kongara, G., He, C., Yang, L., and Armstrong, J. (2019). A comparison of CP-OFDM, PCC-OFDM and UFMC for 5G uplink communications. *IEEE Access*, 7:157574–157594.

Levanen, T., Pirskanen, J., Pajukoski, K., Renfors, M., and Valkama, M. (2019). Transparent Tx and Rx waveform processing for 5G new radio mobile communications. *IEEE Wireless Communications*, 26(1):128–136.

Leyonhjelm, S. and Faulkner, M. (2005). Designing for low ISI in an OFDM modem. In *Proc. IEEE Region 10 Conference (TENCON)*, pages 1–5, Melbourne, Qld., Australia.

Li, F., Zheng, K., Long, H., and Guan, D. (2019). Performance of SCMA with GFDM and FBMC in uplink IoT communications. In *Proc. IEEE Veh. Techn. Conf. (VTC Spring)*, Kuala Lumpur, Malaysia.

Li, J., Bala, E., and Yang, R. (2014). Resource block filtered-OFDM for future spectrally agile and power efficient systems. *Physical Communication*, 14:36–55.

Lin, H. and Siohan, P. (2014). Multi-carrier modulation analysis and WCP-COQAM proposal. *EURASIP J. Advances in Signal Processing*, 2014(1):1–19.

Lin, H. H., Lahbabi, N., Siohan, P., and Jiang, X. (2015). An efficient FTN implementation of the OFDM/OQAM system. In *Proc. IEEE Int. Conf. Commun. (ICC)*, London, UK.

Lopez-Salcedo, J. A., Gutiérrez, E., Seco-Granados, G., and Swindlehurst, A. L. (2013). Unified framework for the synchronization of flexible multicarrier communication signals. *IEEE Trans. Signal Process.*, 61(4):828–842.

Loulou, A. E., Yli-Kaakinen, J., Levanen, T., Lehtinen, V., Schaich, F., Wild, T., Renfors, M., and Valkama, M. (2020). Multiplierless filtered-OFDM transmitter for narrowband IoT devices. *IEEE Internet of Things Journal*, 7(2):846–862.

Mahmoud, H. A. and Arslan, H. (2008). Sidelobe suppression in OFDM-based spectrum sharing systems using adaptive symbol transition. *IEEE Commun. Lett.*, 12(2):133–135.

Mattera, D., Tanda, M., and Bellanger, M. (2016). Filter bank multicarrier with PAM modulation for future wireless systems. *Signal Processing*, 120:594–606.

Matthé, M. and Fettweis, G. (2016). Conjugate root offset-QAM for orthogonal multicarrier transmission. *EURASIP J. Advances in Signal Processing*, 2016(41).

Michailow, N., Matthé, M., Gaspar, I. S., Caldevilla, A. N., Mendes, L. L., Festag, A., and Fettweis, G. (2014). Generalized frequency division multiplexing for 5th generation cellular networks. *IEEE Trans. Commun.*, 62(9):3045–3061.

Muramatsu, S. and Kiya, H. (1997). Extended overlap-add and -save methods for multirate signal processing. *IEEE Trans. Signal Process.*, 45(9):2376–2380.

Muschallik, C. (1996). Improving an OFDM reception using an adaptive Nyquist windowing. *IEEE Trans. Consum. Electron.*, 42(3):259–269.

Nimr, A., Chafii, M., Matthé, M., and Fettweis, G. (2018). Extended GFDM framework: OTFS and GFDM comparison. In *Proc. IEEE Global Commun. Conf. (GLOBECOM)*, Abu Dhabi, UAE.

Nissel, R., Schwarz, S., and Rupp, M. (2017). Filter bank multicarrier modulation schemes for future mobile communications. *IEEE J. Sel. Areas Commun.*, 35(8):1768–1782.

Nouri, M., Lottici, V., Reggiannini, R., Ball, D., and Rayne, M. (2006). TEDS: A high speed digital mobile communication air interface for professional users. *IEEE Veh. Technol. Mag.*, pages 32–42.

Oppenheim, A. and Schafer, R. (1989). *Discrete-Time Signal Processing*. Prentice-Hall.

Pagadarai, S., Rajbanshi, R., Wyglinski, A. M., and Minden, G. J. (2008). Sidelobe suppression for OFDM-based cognitive radios using constellation expansion. In *Proc. IEEE Wireless Commun. Netw. Conf. (WCNC)*, pages 888–893, Las Vegas, NV, USA.

Panta, K. and Armstrong, J. (2003). Spectral analysis of OFDM signals and its improvement by polynomial cancellation coding. *IEEE Trans. Consum. Electron.*, 49(4):939–943.

Pelkowitz, L. (1981). Frequency domain analysis of wraparound error in fast convolution algorithms. *IEEE Trans. Acoust., Speech, Signal Process.*, ASSP-29(3):413–422.

Pérez-Neira, A. I., Caus, M., Zakaria, R., Ruyet, D. L., Kofidis, E., Haardt, M., Mestre, X., and Cheng, Y. (2016). MIMO signal processing in offset-QAM based filter bank multicarrier systems. *IEEE Trans. Signal Process.*, 64(21):5733–5762.

PHYDYAS (n.d.). Physical layer for dynamic spectrum access and cognitive radio. Technical report, FP7-ICT Project 211887 PHYDYAS.

Princen, J. (1995). The design of nonuniform modulated filter banks. *IEEE Trans. Signal Process.*, 43(11):2550–2560.

Pucker, L. (2003). Channelization techniques for software defined radio. In *Proc. Software Defined Radio Technical Conf. (SDR)*, Orlando, FL, USA.

Qualcomm (2015). *5G Waveform and Multiple Access Techniques*. Qualcomm Technologies, Inc.

Rabiner, L. R. and Gold, B. (1975). *Theory and Application of Digital Signal Processing*. Englewood Cliffs, NJ: Prentice-Hall.

Renfors, M. and f. harris (2011). Highly adjustable multirate digital filters based on fast convolution. In *Proc. European Conf. Circuit Theory Design (ECCTD)*, pages 9–12, Linköping, Sweden.

Renfors, M., Mestre, X., Kofidis, E., and Bader, F., editors (2017). *Orthogonal Waveforms and Filter Banks for Future Communication Systems*. Academic Press.

Renfors, M. and Yli-Kaakinen, J. (2013). Timing offset compensation in fast-convolution filter bank based waveform processing. In *Proc. IEEE Int. Symp. Wireless Commun. Syst. (ISWCS)*, Ilmenau, Germany.

Renfors, M. and Yli-Kaakinen, J. (2014). Channel equalization in fast-convolution filter bank based receivers for professional mobile radio. In *Proc. European Wireless Conf. (EW)*, Barcelona, Spain.

Renfors, M., Yli-Kaakinen, J., and Harris, F. (2014). Analysis and design of efficient and flexible fast-convolution based multirate filter banks. *IEEE Trans. Signal Process.*, 62(15):3768–3783.

Renfors, M., Yli-Kaakinen, J., Levanen, T., and Valkama, M. (2016). Fast-convolution filtered OFDM waveforms with adjustable CP length. In *Proc. IEEE Global Conf. Signal Inform. Process. (GlobalSIP)*, Greater Washington, DC, USA.

Renfors, M., Yli-Kaakinen, J., Levanen, T., Valkama, M., Ihalainen, T., and Vihriälä, J. (2015). Efficient fast-convolution implementation of filtered CP-OFDM waveform processing for 5G. In *Proc. IEEE Global Commun. Conf. (GLOBECOM)*, San Diego, CA, USA.

Sahin, A. and Arslan, H. (2011). Edge windowing for OFDM based systems. *IEEE Commun. Lett.*, 15(11):1208–1211.

Saltzberg, B. R. (1967). Performance of an efficient parallel data transmission system. *IEEE Trans. Commun. Technol.*, 15(6):805–811.

Shao, K., Alhava, J., Yli-Kaakinen, J., and Renfors, M. (2015). Fast-convolution implementation of filter bank multicarrier waveform processing. In *Proc. IEEE Int. Symp. Circuits Syst. (ISCAS)*, Lisbon, Portugal.

Shao, K., Pi, L., Yli-Kaakinen, J., and Renfors, M. (2017). Filtered multitone multicarrier modulation with partially overlapping sub-channels. In *Proc. EURASIP European Signal Process. Conf. (EUSIPCO)*, pages 405–409, Kos island, Greece.

Siohan, P., Siclet, C., and Lacaille, N. (2002). Analysis and design of OFDM/OQAM systems based on filterbank theory. *IEEE Trans. Signal Process.*, 50(5):1170–1183.

Stockham, Jr., T. G. (1966). High-speed convolution and correlation. In *Proc. AFIPS Spring Joint Computer Conference*, volume 28, pages 229–233, Boston, MA, USA.

Tonello, A. M. (2003). Asynchronous multicarrier multiple access: Optimal and suboptimal detection and decoding. *Bell. Syst. Tech. J.*, 7(3):191–217.

Tonello, A. M. (2006). A concatenated multitone multiple-antenna air-interface for the asynchronous multiple-access channel. *IEEE J. Sel. Areas Commun.*, 24(3):457–469.

Tzannes, M. A., Tzannes, M. C., Proakis, J., and Heller, P. N. (1994). DMT systems, DWMT systems and digital filter banks. In *Proc. IEEE Int. Conf. Commun. (ICC)*, volume 1, pages 311–315, New Orleans, USA.

Umehira, M. and Tanabe, M. (2010). Performance analysis of overlap FFT filter-bank for dynamic spectrum access applications. In *Proc. Asia-Pacific Conf. Commun. (APCC)*, pages 424–428, Auckland, New Zealand.

Vakilian, V., Wild, T., Schaich, F., ten Brink, S., and Frigon, J. F. (2013). Universal-filtered multi-carrier technique for wireless systems beyond LTE. In *Proc. IEEE Globecom Workshops (GC Wkshps)*, pages 223–228, Atlanta, GA, USA.

Vallet, R. and Taieb, K. H. (1995). Fraction spaced multi-carrier modulation. *Wireless Personal Communications*, 2:97–103.

Wang, S., Thompson, J. S., and Grant, P. M. (2017). Closed-form expressions for ICI/ISI in filtered OFDM systems for asynchronous 5G uplink. *IEEE Trans. Commun.*, 65(11):4886–4898.

Weiss, T., Hillenbrand, J., Krohn, A., and Jondral, F. K. (2004). Mutual interference in OFDM-based spectrum pooling systems. In *Proc. IEEE Veh. Techn. Conf. (VTC Spring)*, volume 4, pages 1873–1877, Milan, Italy.

Wild, T. and Schaich, F. (2015). A reduced complexity transmitter for UF-OFDM. In *Proc. IEEE Veh. Techn. Conf. (VTC Spring)*, Glasgow, UK.

Yli-Kaakinen, J., Levanen, T., Palin, A., Renfors, M., and Valkama, M. (2020). Generalized fast-convolution-based filtered-OFDM: Techniques and application to 5G new radio. *IEEE Trans. Signal Process.*, 68:1213–1228.

Yli-Kaakinen, J., Levanen, T., Renfors, M., Valkama, M., and Pajukoski, K. (2018). FFT-domain signal processing for spectrally-enhanced CP-OFDM waveforms in 5G New Radio. In *Proc. Asilomar Conf. Signals Syst. Comput. (ACSSC)*, pages 1049–1056, Pacific Grove, CA, USA.

Yli-Kaakinen, J., Levanen, T., Valkonen, S., Pajukoski, K., Pirskanen, J., Renfors, M., and Valkama, M. (2017). Efficient fast-convolution-based waveform processing for 5G physical layer. *IEEE J. Sel. Areas Commun.*, 35(6):1309–1326.

Yli-Kaakinen, J. and Renfors, M. (2015). Flexible fast-convolution implementation of single-carrier waveform processing. In *Proc. IEEE Int. Conf. Commun., ICC2015 Workshops*, London, U.K.

Zakaria, R. and Le Ruyet, D. (2010). On maximum likelihood MIMO detection in QAM-FBMC systems. In *Proc. IEEE Int. Symp. Personal, Indoor, Mobile Radio Commun. (PIMRC)*, Istanbul, Turkey.

Zakaria, R. and Le Ruyet, D. (2012). A novel filter-bank multicarrier scheme to mitigate the intrinsic interference: Application to MIMO systems. *IEEE Trans. Wireless Commun.*, 11(3):1112–1123.

Zayani, R., Medjahdi, Y., Shaiek, H., and Roviras, D. (2016). WOLA-OFDM: a potential candidate for asynchronous 5G. In *2016 IEEE Globecom Workshops (GC Wkshps)*, pages 1–5.

Zayani, R., Shaiek, H., Cheng, X., Fu, X., Alexandre, C., and Roviras, D. (2018). Experimental testbed of post-OFDM waveforms toward future wireless networks. *IEEE Access*, 6:67665–67680.

Zhang, C. and Wang, Z. (2000). A fast frequency domain filter bank realization algorithm. In *Proc. Int. Conf. Signal Process. (ICSP)*, volume 1, pages 130–132, Beijing, China.

Zhang, L., Ijaz, A., Xiao, P., Molu, M. M., and Tafazolli, R. (2018). Filtered OFDM systems, algorithms, and performance analysis for 5G and beyond. *IEEE Trans. Commun.*, 66(3):1205–1218.

Zhang, X., Jia, M., Chen, L., Ma, J., and Qiu, J. (2015). Filtered-OFDM – Enabler for flexible waveform in the 5th generation cellular networks. In *Proc. IEEE Global Commun. Conf. (GLOBECOM)*, pages 1–6, San Diego, CA, USA.

Zhao, Z., Schellmann, M., Wang, Q., Gong, X., Boehnke, R., and Xu, W. (2015). Pulse shaped OFDM for asynchronous uplink access. In *Proc. Asilomar Conf. Signals Syst. Comput. (ACSSC)*, pages 3–7, Pacific Grove, CA, USA.

ABSTRACT

Orthogonal frequency-division multiplexing (OFDM) has been adopted as the waveform of choice in existing and emerging broadband wireless communication systems for a number of advantages it can offer. Nevertheless, investigations of more advanced multicarrier transmission schemes have continued with the aim of eliminating or mitigating its essential limitations. This chapter discusses multicarrier schemes with enhanced spectrum localization, which manage to reduce the spectral sidelobes of plain OFDM that are problematic in various advanced communication scenarios. These include schemes for enhancing the OFDM waveform characteristics through additional signal processing, as well as filter-bank multicarrier (FBMC) waveforms utilizing frequency-selective filter banks instead of plain (inverse) discrete Fourier transform processing for waveform generation and demodulation.

KEYWORDS

multicarrier; filtered orthogonal frequency-division multiplexing (F-OFDM); filter bank; filter-bank multicarrier with offset-quadrature amplitude modulation (FBMC/OQAM); filtered multitone (FMT); generalized frequency-division multiplexing (GFDM); fast convolution; windowed overlap-and-add (WOLA); universally filtered multicarrier (UFMC); fifth generation (5G) new radio